the underground structure. For this successful waterproof mechanism, the grout material has ability to flow well in rock fracture and to achieve proper strength after curing.

Therefore, in order to economical and efficient design of rock grouting in deep depth, the performance should be verified according to grout property, geometry of fracture, and underground ambient environmental conditions such as water saturation level or temperature (Gustafson 1996, Sui 2015).

Several researchers have studied the efficiency in grouting the fractured rock and its relationship with the grout penetration into the individual fractures. Eriksson (2002) concluded that the aperture size, its variation and geometrical measures are the important factors affecting the grout penetrability. Draganovic (2011) also suggested that many factors such as grout pressure, density and the geometry of constriction can influence the complex process of the injected grout penetration. Effect of flowing water on grouting in fractured rock was experimentally investigated by Zhang (2011). Carter (2012) proposed a grouting closure standard based on conductivities at different grouting stages. Sui (2015) evaluated the relationship between sealing efficiency and influencing factors such as fracture aperture width, initial water speed, gel time and grout take in single fracture model.

In this study, grouting injection tests were performed using micro cement grout with a transparent fracture replica with various aperture sizes in the laboratory. Given experimental data, penetration pattern of grouting was analyzed; factor affecting the waterproof efficiency was evaluated for better understanding of grout flow in rock fracture. In addition, the phenomena of air bubbles and bleeding during injection or curing of grouts were discussed for the successful performance of rock grouting. The results of this study can provide the basic knowledge to determine the efficiency of waterproof for rock grouting in deep depth

2. MATERIALS AND METHODS

2.1 Test set-up

Fig. 1 shows an experimental set-up for grout injection and permeability test in deep underground conditions. It is composed of five parts which are syringe pump, high-pressure water pump, multichannel data acquisition, test section, and digital camera.

Fig. 1 Picture of experimental set-up. (1 – Syringe pump; Accurate high-pressure pump; 3 – Multichannel data acquisition and control box; 4 – Test section; 5 – Digital camera).

In this experiment, the syringe pump was used for injecting grouts into artificial fracture. The dynamic flow rate provided by the syringe pump could reach 6000 mL/min. High-pressure water pump was used to estimate permeability and waterproof efficiency after rock grouting. It can provide the high water pressure up to 100 bars. Multichannel data system was installed for controlling experimental parameters and acquiring data. Using display system, we regulated the injection conditions of pumps such as injection pressure and flow rate of fluid materials. Also, the feedback system can optimize and stabilize the injection condition. A digital camera was used to visually observe and record the penetration and distribution of injected grouts. This visual device has a display resolution of 4608 × 3288 (15 millions) and can record the moving images at 7 frames per second.

2.2 Specimen preparation

Micro cements are often used for improving strength of a poor rock and preventing ground water inflow into underground space. In deep depth conditions, the aperture sizes of individual fractures are very small due to high in-situ stress. Thus, ordinary cement has limitation for injecting grouts into fine rock joint. For this reason, the grout material selected for our experiments is MICEM 8000 (micro cement) manufactured by SsangYong cement in Korea. Fig. 2 and Table 1 indicate grain size distribution and physical properties of MICEM 8000 used in this study.

Table 1 Physical properties of micro grout (MICEM 8000).

Property	Value
Specific gravity (-)	2.95
Particle size of D_{95} (μm)	< 16
Average particle size (μm)	4 ~ 6

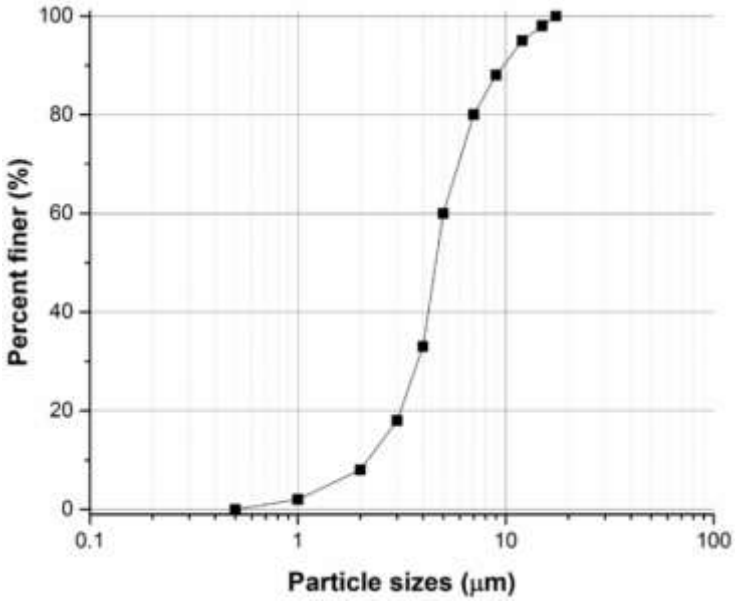

Fig. 2 Grain size distribution curve of micro grout (MICEM 8000).

The micro cement used in this study has a D_{95} of less than 16 μm from grain size distribution and specific gravity of 2.95. Water cement mixed ratio (W/C ratio) is important factor characterizing the viscous fluid flow in rock fractures. Previous studies mainly used the W/C ratio range from 0.5 to 1.0 (e.g., Chun 2005, Høien 2014, Rahman 2015). Considering the bleeding and fluidity of grouts, the W/C ratio was selected as 1.0 to have good fluidity in this study (Fig. 3). The chemical additives for hardening and improving grouts were not considered in this experiment.

Fig. 3 Material (micro cement) used for grouting injection.

Fig. 4 shows a test cell for evaluating the penetration patterns and waterproof efficiency of rock grouting at deep depth conditions. The cell was specially designed rectangular acrylic parallel plane model and has the fracture size of 200 mm (width) × 400 mm (length) with different apertures (1, 5, and 10 mm). International Society for Rock Mechanics suggested that the fracture with aperture between 0.5 and 10 mm are a possible pathway flowing water in grouting practice (ISRM 1978). Thus, the fracture cell with aperture size: 1 – 10 mm were selected and used in this experiment. The ports are

composed of grouts injection point (B), water injection and drainage point for initial water saturation conditions of describing deep underground space and the permeability estimation (A and C). Inner diameter of all ports and distance between ports are 0.95 mm (3/8 inches), 180 mm respectively. The boundary of cell was perfectly sealed and thus injected water and grouts can only migrate through ports.

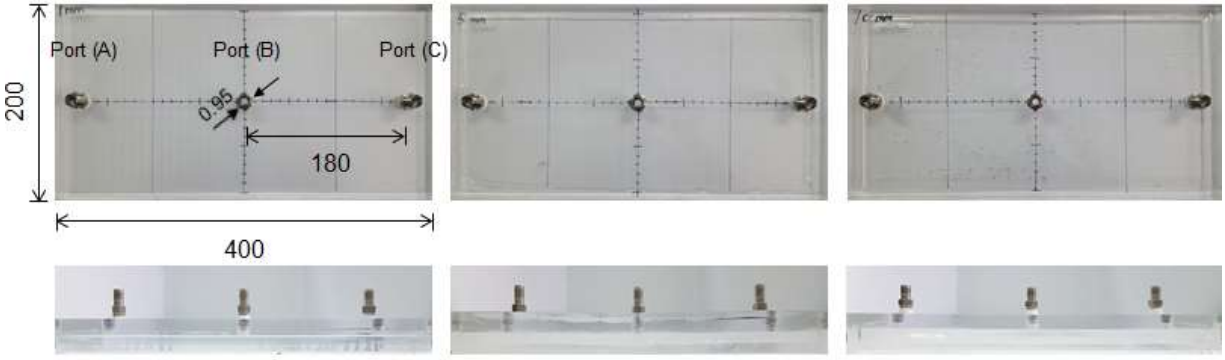

Fig. 4 Test cells of artificial fracture with different aperture and inlet/outlet port: (a) 1 mm, (b) 5 mm, and (c) 10 mm apertures.

2.3 Test process

For injecting grout material, the micro cement was mixed with water under constant condition (W/C ratio = 1.0). The mixtures were sufficiently stirred during 30 minutes under temperature condition of 21 ± 1°C for preventing separation between micro cement and water before injection. To simulate saturated rock fractures by groundwater in deep underground environment, the fracture cell was fully saturated with tap water. Grouts with flow rate of 200 ml/min were injected into port (B) using syringe pump. Port (A) and (C) were open because they acted as outlet during grouting injection process. Additionally, the grouts were continuously injected until the injected grouts was pushed out to port (A) and (C) for the perfect saturation condition of grouts inside the fracture cell. We measured a spreading velocity and distribution of grouts using digital camera. After grouting, all ports were sealed for preventing the external influences while the grouts were cured. The curing process proceeded during 7 days under constant temperature of 21 ± 1°C. Finally, permeability tests were conducted in the grouted fractures for evaluating the waterproof efficiency of grouting using high-pressure water pump. Grouts injection port (B) was closed and the port (A) and (C) were set as inlet and outlet for estimating water permeability, respectively. For estimating permeability after curing process, the outflow water at port (C) was collected and measured according to the elapsed time

3. RESULTS AND ANALYSIS

3.1 Grout penetration patterns

Fig. 5 shows grout propagation during into the fracture with various aperture sizes. Parallel acrylic fractures were initially filled with water. There was no water flow within fractures and this static water condition was maintained during grout injection tests. In

case of 10 mm aperture size, the propagation for static water grouting was round in shape during the first 14 second before the grout reached the fracture side boundary (Fig. 5a). A slight dilution was visually identified at the between grout body and saturated water. In case of 5 mm aperture size, abnormal propagation pattern was observed near the central injection hole due to trapped air (Fig. 5b). In two cases (5 and 10 mm aperture sizes), circular grout front was commonly observed at the early stage of the grout injection tests.

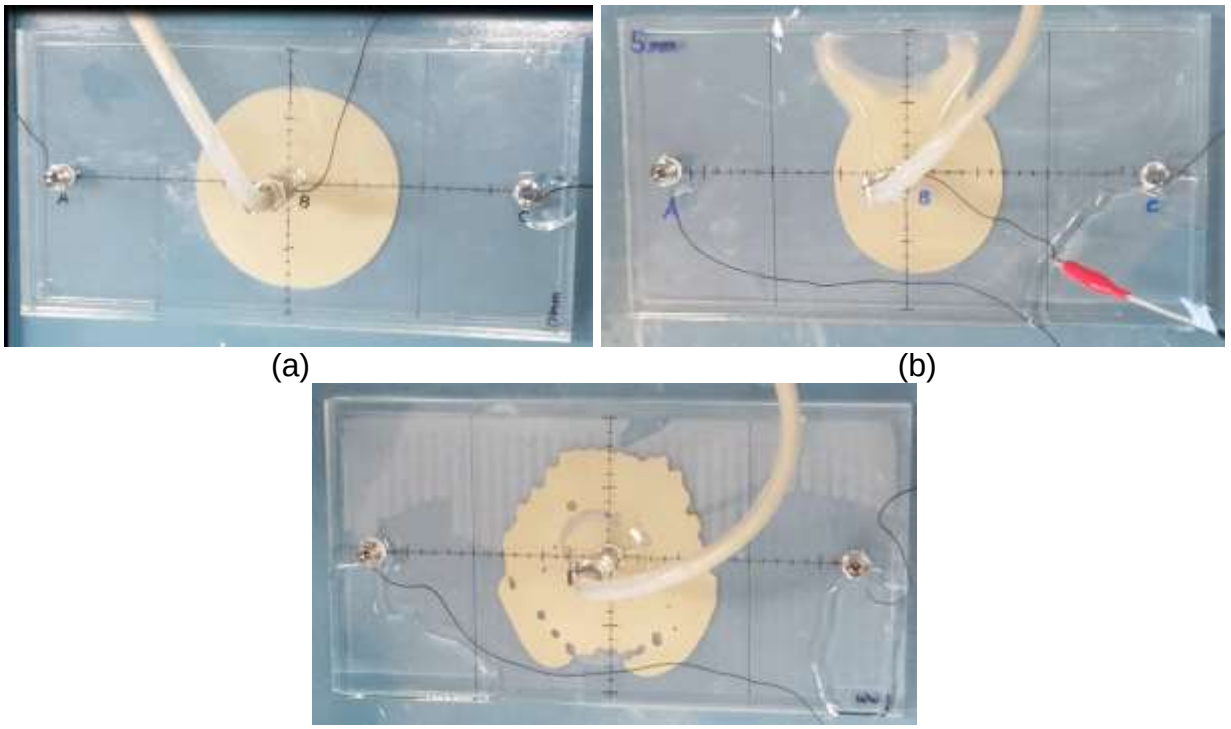

(a) (b)

(c)

Fig. 5 Propagation of grouts: (a) 10 mm, (b) 5 mm, and (c) 1 mm apertures.

In case of small fracture with 1 mm aperture size, the grout radially spreads to both the boundaries of the fracture, but the stratigraphic penetration pattern occurs partially due to the micro-fine furrows and ridges within fracture by the manufacturing process of micro-fracture (Fig. 5c). Although there were local differences of grout moving behavior, the similar radial penetration pattern was generally identified in all three cases.

However, under the condition of constant grout injection rate (200 ml/min), the speed of grout penetrations showed clear distinction according to the aperture sizes. In each experimental case, the speed of grout penetrations was estimated using the penetration distance over the elapsed time.

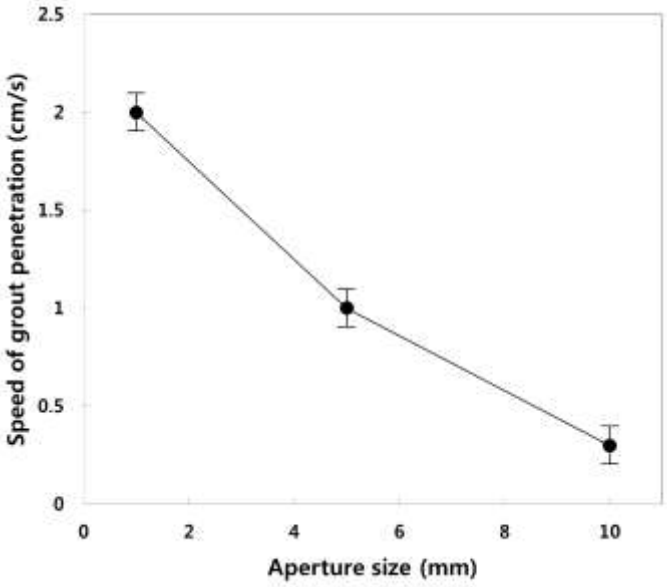

Fig. 6 Speed of grout penetration versus aperture size.

The speed of grout penetrations were 2 cm/s, 1 cm/s and 0.3 cm/s in cases of 1, 5 and 10 mm aperture sizes, respectively. Fig. 6 shows the speed of grout penetrations versus the various aperture-fractures. As the aperture size was increased, the speed of grout penetrations was decreased. The speed of grout penetration was inversely proportional to aperture sizes, which corresponds with the results of the analytical solution suggested by Gustafson (1996).

3.2 Influencing factor on waterproof ability

To evaluate the waterproof efficiency of grouting, the permeability tests were conducted after curing process. Waterproof efficiency (*WE*) adopted is defined as the reduction of the cross-fracture flow due to the grouting performance and can be estimated as follows:

$$WE\ (\%) = (Q_0 - Q_{grouted}) / Q_0 \cdot 100 \quad (1)$$

where Q_0 is the initial water flow rate before grouting and $Q_{grouted}$ is the water flow rate after grouting. These values were commonly measured in the outlet port of the fracture. Fig. 7 shows the waterproof efficiency according to the aperture sizes. In case of 1 mm aperture size, the waterproof efficiency was obtained to be 100% after grouting process.

This means that there was no flow and leakage through fractures due to grouting in this case, indicating the excellent waterproof efficiency of grouting. Any crack or water leakage was not observed even at the extreme high pressure (> 100 bars) of the water injected for evaluating permeability. This implies that the sealing effect of rock grouting is maintained under the deep depth condition (≈ 1 km) in case of micro-fracture with 1 mm aperture size. In two cases (5 and 10 mm aperture sizes), the waterproof efficiency were 79.4% and 61.2% after grouting process, respectively.

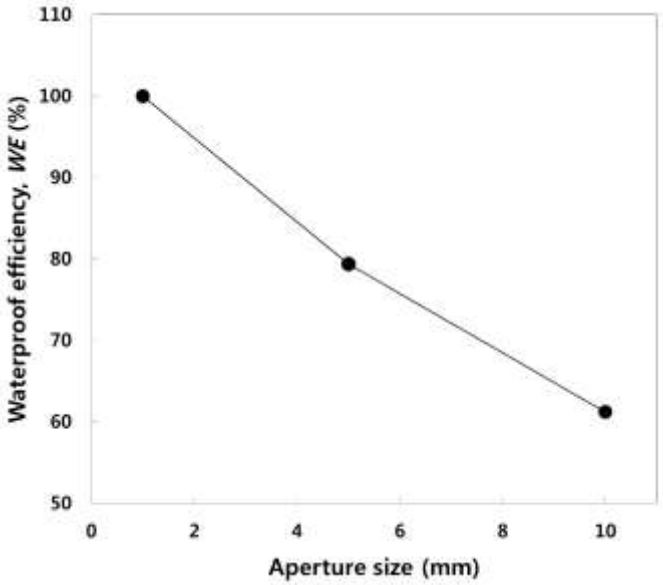

Fig. 7 Waterproof efficiency (*WE*) versus aperture size.

Although the fracture inside was mostly filled with the injected grouts at the 5 mm and 10 mm aperture, the empty spaces were widely formed at the upper part of fracture channel, which caused the water flow even after the grout curing. Moreover, the waterproof efficiency was decreased as the aperture size was increased (Fig. 7).

4. DISCUSSIONS

When the grout is injected into the fracture, the air bubble can be formed due to the mixing and injection processes. In this study, many air bubbles was observed and separately located in the fracture inside as shown in Fig. 8.

Fig. 8 An example of air bubble occurrence in the grouted fracture.

To evaluate the effect of the air bubbles on leakage or water permeability after grouting, the high pressure water over 100 bars was injected into the grouted fracture.

Consequently, the separated air bubbles as the closed pores do not affect the short-term permeability of fractures sealed by grouting. However, in case of the grout injection with high pressure at deep depth, more air bubbles may occur due to the formation of turbulent flow. This can induce water leakage of the grouted fractures by creating continuous pores. Moreover, the air bubbles may become large water pathway if the grouting is corroded or deformed in the long-term, which can greatly reduce the grouting efficiency.

Bleeding usually occurs in the direction of gravity during the curing process after the fracture aperture is fully filled with the injected grouts. This bleeding phenomenon causes the empty space at the upper part of fracture aperture. In this study, there was no gap between the aperture channel and the cured grouts in case of 1 mm aperture. In both cases of 5 and 10 mm apertures, the bleedings were observed at the upper part of fracture channel. The ratios of empty space by bleeding to total apertures were 7.4% and 15.2%, respectively. From this result, it can be inferred that the bleeding phenomenon may be intensified as the aperture size increases. The mixing ratio of water and cement (*W/C*) as well as the aperture size can influence the extent of bleeding. If the ratio value is less than 1.0, the bleeding may be considerably reduced.

Therefore, the phenomena of air bubbles and bleeding during injection or curing of grouts are major factors decreasing the waterproof ability of grouting. The methods that minimize these two factors will be needed for the successful performance of rock grouting. In this respect, we are preparing an expanded research about the various other effects of the grout mixing ratio, ambient flow velocity and high temperature on air bubbles and bleeding phenomena in real rock fractures.

5. CONCLUSIONS

In this study, we evaluated the factor affecting the waterproof efficiency and penetration pattern of rock grouting through the laboratory experiments using a transparent fracture replica with various aperture sizes. Main conclusions from our experiments were as follows:

1) Grouts penetration patterns were commonly radial form in all three cases. Under constant condition of grout injection rate (200 ml/min) and *W/C* (1.0), The speed of grout penetrations were 2 cm/s, 1 cm/s and 0.3 cm/s at fractures with apertures of 1 mm, 5 mm, and 10 mm, respectively. The speed of grout penetration was inversely proportional to aperture sizes.
2) The waterproof efficiency was estimated to be 100%, 79.4% and 61.2% after grouting process at fractures with apertures of 1 mm, 5 mm and 10 mm, respectively. As the aperture size was increased, the waterproof efficiency was decreased.
3) Air bubbles and bleeding phenomena should be considered in rock grouting construction because they reduce the waterproof ability under a deep depth condition.

ACKNOWLEDGEMENT

This study was supported by the Basic Research and Development Project of the Korea Institute of Geoscience and Mineral Resources (KIGAM), which was funded by the Ministry of Science, ICT and Future Planning, Korea. The authors would like to thank an anonymous reviewer for his/her valuable and constructive comments in revising the manuscript.

REFERENCES

Carter, T.G., Dershowitz, W., Shuttle, D. and Jefferies, M. (2012), “Improved methods of design for grouting fractured rock. In: Lawrence, F.J., Donald, A.B. and Michael, J.B. (Eds.), Grouting and Deep Mixing 2012”, Geotechnical Special Publications (GSP).

Chun, B.S., Kim, D.Y. and Lee, Y.N. (2002), “Shear characteristic of the cement grouted sawtoothed joints”, *J. Korean Soc. Civil Eng.*, Vol. **22**(5C), 469-478.

Draganovic, A. and Stille, H. (2011), “Filtration and penetrability of cement-based grout: Study performed with a short slot”, *Tunn. Undergr. Space Technol.,* Vol. **26**(4), 548-559.

Eriksson, M. (2012), “Prediction of grout spread and sealing effect: A probabilistic approach”, UMI Dissertations Publishing.

Gustafson, G. and Stille, H. (1996), “Prediction of groutability from grout properties and hydrogeological data”, *Tunn. Undergr. Space Technol.,* Vol. **11**(3), 325-332.

Høien, A.H. and Nilsen, B. (2014), “Rock mass grouting in the Løren tunnel: Case study with the main focus on the groutability and feasibility of drill parameter interpretation”, *Rock Mech. Rock Eng.*, Vol. **47**(3), 967-983.

ISRM. (1978), “Suggested methods for the quantitative description of discontinuities in rock masses”, *Int. J. Rock Mech. Min. Sci & Geomech.*, Vol. **15**(6), 319-368.

Mohammed, M.H., Pusch, R. and Knutsson, S. (2015), “Study of cement-grout penetration into fractures under static and oscillatory conditions”, *Tunn. Undergr. Space Technol.,* Vol. **45**, 10-19.

Rahman, M., Håkansson, U. and Wiklund, J. (2015), In-line rheological measurements of cement grouts: Effects of water/cement ratio and hydration”, *Tunn. Undergr. Space Technol.,* Vol. **45**, 34-42.

Sui, W., Liu, J., Hu, W., Qi, J. and Zhan, K. (2015), “Experimental investigation on sealing efficiency of chemical grouting in rock fracture with flowing water”, *Tunn. Undergr. Space Technol.,* Vol. **50**, 239-249.

Zhang, G., Zhan, K., Gao, Y. and Wang, W. (2011), “Comparative experimental investigation of chemical grouting into a fracture with flowing and static water”, *Min. Sci. Technol. (China).,* Vol. **21**, 201-205.